Thermal-light full-field optical coherence tomography

Laurent Vabre, Arnaud Dubois, Claude Boccara

Thermal-light full-field optical coherence tomography

L. Vabre, A. Dubois, and A. C. Boccara

Laboratoire d'Optique Physique, Ecole Supérieure de Physique et de Chimie Industrielles, Centre National de la Recherche Scientifique, Unité Propre de Recherche A0005, 10 Rue Vauquelin, 75005 Paris, France

Received November 1, 2001

We have built a high-resolution optical coherence tomography (OCT) system, based on a Linnik-type interference microscope, illuminated by a white-light thermal lamp. The extremely short coherence length of the illumination source and the large aperture of the objectives permit resolution close to 1 μm in three dimensions. A parallel detection scheme with a CCD camera provides cross-section ($x-y$) image acquisition without scanning at a rate of up to 50 Hz. To our knowledge, our system has the highest resolution demonstrated to date for OCT imaging. With identical resolution in three dimensions, realistic volume rendering of structures inside biological tissues is possible. © 2002 Optical Society of America

OCIS codes: 110.4500, 170.6900, 180.3170, 170.3880.

Optical coherence tomography (OCT) is an emerging three-dimensional (3D) imaging technique with micrometer-scale resolution.[1] The method has seen many improvements to increase the image resolution and sensitivity for biological tissue investigations.[2] OCT has been applied clinically for *in vivo* cross-section imaging inside various tissues, such as human retina,[3] skin,[4] and gastrointestinal structures.[5] Extensions of conventional OCT have been developed to measure birefringence,[6] to obtain spectroscopic information,[7] and to image the flow velocity of moving particles (Doppler OCT).[8]

Most OCT systems are based on a fiber-optic Michelson interferometer illuminated by a broad-bandwidth source. The longitudinal (z) resolution is governed by the coherence length of the illumination source, which depends on the spectral bandwidth. Superluminescent diodes were the first sources used for OCT, leading to typically 10–15-μm longitudinal resolution. OCT systems using femtosecond lasers were then proposed to improve longitudinal resolution. To the best of our knowledge, the highest 3D resolution published to date was 1 μm $\times$ 3 μm (longitudinal $\times$ transverse), obtained with state of the art broad-bandwidth femtosecond laser technology.[9] Recently, similar resolutions have been obtained with tungsten halogen and xenon lamps.[10] OCT images are usually recorded in an ($x-z$) cross section. The interference signal is detected by a single detector, and the full images are recorded point by point with a fast two-dimensional scanning system. Limitations resulting from the depth of field (z direction) are avoided by use of low-N.A. optics, which consequently limits lateral resolution. One can, however, use zone-focusing and image-fusion techniques to maintain good transverse resolution at varying depths through the image.[9] To avoid lateral scanning, Bourquin *et al.*[11] have recently developed a smart detector array. Beaurepaire *et al.*[12] also proposed an alternative solution to produce en-face ($x-y$) tomographic images without scanning, using a Linnik polarization microscope associated with a CCD array and stroboscopic illumination with a LED. The longitudinal resolution of this system, governed by the coherence length of the LED, was close to 10 μm.

To improve the longitudinal resolution of the system, we have built a new setup that uses a broadband white-light thermal lamp. The system is based on the Linnik interference microscope geometry (see Fig. 1) with a 100-W tungsten halogen lamp in a Köhler illumination system. The interference images are digitized by a CCD camera (256 $\times$ 256 pixels, 8 bits) working at a maximum rate of 200 frames/s. The image acquisitions, calculations, and display are realized by means of homemade software.

A piezoelectric transducer supporting the reference mirror creates a sinusoidal phase modulation with an amplitude of 2.45 at the frequency $f = 50$ Hz (see Fig. 1).[13] The signal to be extracted is the interference fringe intensity corresponding to the light that is backscattered from a particular slice inside the sample.

The piezoelectric transducer oscillates at a frequency chosen to be exactly a quarter of the

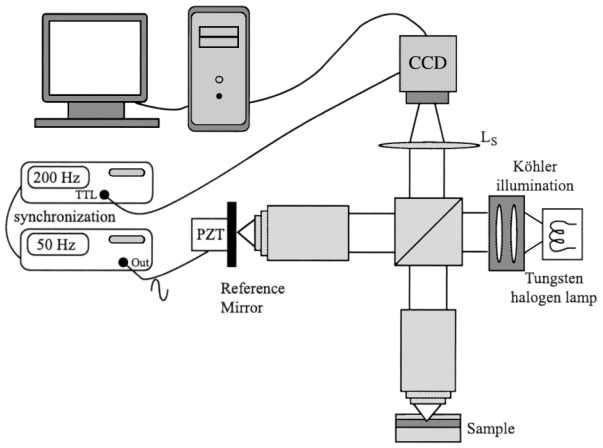

Fig. 1. Schematic of the interference microscope, which is based on a Michelson interferometer with identical water-immersion microscope objectives in both arms. The interference images are recorded by a CCD camera. PZT, piezoelectric transducer; Out., sinusoidal output.

0146-9592/02/070530-03$15.00/0

image-acquisition rate. The modulation and image acquisition are synchronized and phase locked. Four images, $S_{0,1,2,3}$, are recorded during each modulation period. The tomographic image, A, is calculated with the following formula[13]:

$$A = [(S_0 - S_1 - S_2 + S_3)^2 + (S_0 - S_1 + S_2 - S_3)^2]^{1/2}. \quad (1)$$

The thickness of the observed slice is actually determined by the product of the source spectrum by the spectral response of the CCD (peak at $\lambda = 840$ nm, bandwidth $\Delta\lambda \sim 260$ nm). Figure 2 shows the measured axial response of the complete system (source + CCD). Defining the axial resolution as the FWHM of the envelope of this interferogram, we obtain an axial resolution close to 1.2 μm. This measure is obtained by use of a mirror shifted in the axial direction as the observed object. Care must be taken with a biological sample, because spectral dispersion will degrade the axial resolution. For instance, we have observed that after passing through 0.1 mm of glass (single pass), the coherence length is enlarged by a factor of 2. To avoid this phenomenon, we employ water-immersion objectives. The dispersion is then minimized whatever the depth of the observed slice of tissue. Moreover, the unwanted specular reflection at the tissue surface is eliminated.

The lateral resolution is ultimately limited by the N.A. of the objectives. With 0.3-N.A. water-immersion objectives and an average wavelength of 0.8 μm, the lateral resolution is close to 1.3 μm. We note that the lateral resolution will also deteriorate with depth when we are imaging through scattering media because of the detection of multiply scattered light,[14] the aperture reduction effect of the focused beam,[15] and optical aberrations.

We define the sensitivity of our detection scheme as the ratio of the maximal signal to the smallest detectable one. For exposure times of ~1 s (sum of 50 images acquired at 50 Hz), the sensitivity of our system is close to 80 dB. This value is lower than that of recent laser-based OCT systems.[9] This lower value is due to the low brightness of our illumination source compared with that of lasers and to the low dynamic range of our CCD sensor compared with those of photomultiplier tubes or photodiodes. This limit will reduce the maximum investigated depth to a few hundred micrometers. However, our system has a higher lateral resolution. It is more compact and less expensive than systems based on ultrashort pulsed lasers. These advantages are of great interest if there is no need for a large penetration depth.

Figure 3 shows a 3D reconstruction of a *Xenopus laevis* tadpole eye. We recorded 300 tomographic images (x–y) for the reconstruction by moving the sample axially in steps of 1 μm. The exposure time for each image was 1 s. Different structures such as the crystalline lens and the exterior of the eye are very well revealed. The cornea is also visible but with a much lower contrast than the crystalline lens. This lower contrast is due to the fact that the refractive index of the cornea is close to that of water. The refractive index of the crystalline lens is higher because it realizes the focalization inside the tadpole eye. Four of these images are shown in Fig. 4: the cornea surface, the top and bottom of the crystalline lens, and a cut showing the exterior and the crystalline lens.

To our knowledge, this is the first time that an axial resolution close to 1 μm inside biological tissues has been obtained by use of a cheap illumination source. The resolutions in the three dimensions are very close, which permits realistic volume reconstructions. The use of a thermal lamp is of great interest because of its extremely short coherence length at a very low price. The intensity is very stable and the spatial incoherence avoids speckle formation in the images. The major

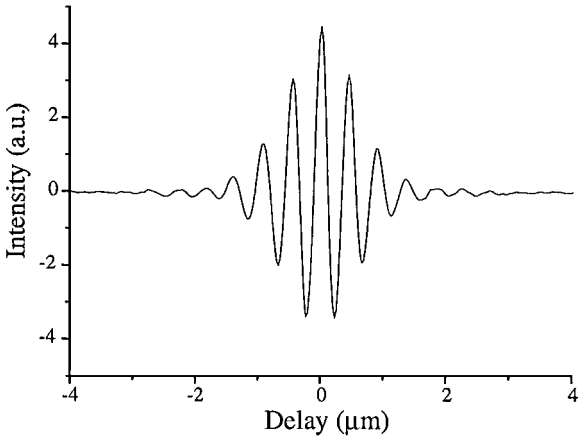

Fig. 2. Measured longitudinal responses of the complete system. The FWHM is 1.3 μm.

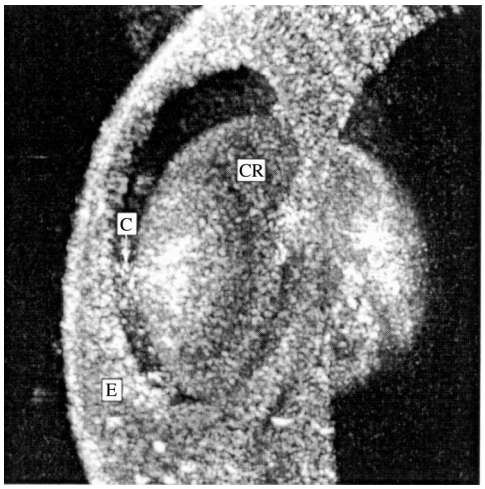

Fig. 3. 3D reconstruction of a *Xenopus laevis* tadpole eye by means of 300 tomographic images. The volume is 360 μm × 360 μm × 200 μm. E, exterior of the eye; C, cornea; CR, crystalline lens.

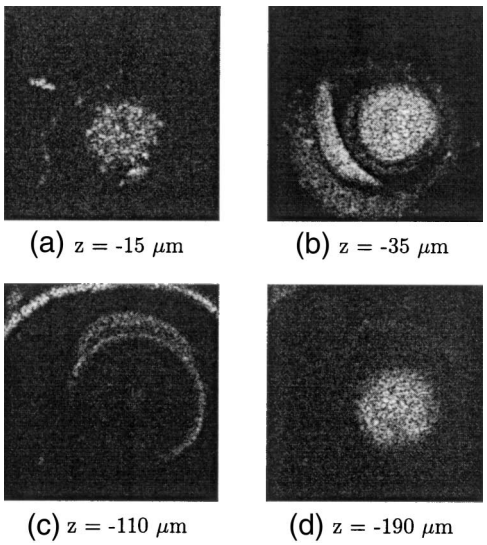

Fig. 4. Examples of tomographic images of the tadpole eye at different depths: (a) cornea, (b) crystalline lens surface and the beginning of the exterior of the eye, (c) exterior of the eye and the crystalline lens, (d) back of the crystalline lens. Field of view, 360 μm $\times$ 360 μm. Exposure time, 1 s.

drawback, however, is the low brightness, which limits the sensitivity of the microscope.

The authors thank E. Beaurepaire for fruitful discussions. We are grateful to V. Reita and P. Piart for mechanical conception and realization and to F. Lejeune and F. Cassagne for electronic realizations and support. L. Vabre is grateful to the Délégation Générale pour l'Armement. This work was supported by the Centre National de la Recherche Scientifique. L. Vabre's e-mail address is vabre@optique.espci.fr.

References

1. D. Huang, E. A. Swanson, C. P. Lin, J. S. Schuman, W. G. Stinson, W. Chang, M. R. Hee, T. Flotte, K. Gregory, C. A. Puliafito, and F. G. Fujimoto, Science **254,** 1178 (1991).
2. J. Izatt, M. R. Hee, G. Owen, E. A. Swanson, and J. G. Fujimoto, Opt. Lett. **19,** 590 (1994).
3. E. A. Swanson, J. A. Izatt, M. R. Hee, D. Huang, C. P. Lin, J. S. Schunen, C. A. Puliafito, and F. G. Fujimoto, Opt. Lett. **18,** 1864 (1993).
4. C. E. Saxer, J. F. de Boer, B. H. Park, Y. Zhao, Z. Chen, and J. S. Nelson, Opt. Lett. **25,** 1355 (2000).
5. A. M. Rollins, R. Ung-Arunyawee, A. Chak, C. K. Wong, K. Kobayashi, M. V. Sivak, Jr., and J. A. Izatt, Opt. Lett. **24,** 1358 (1999).
6. M. J. Everett, K. Schoenenberger, B. W. Colston, and L. B. Da Silva, Opt. Lett. **23,** 228 (1998).
7. U. Morgner, F. X. Kartner, X. D. Li, C. Pitris, E. P. Ippen, and J. G. Fujimoto, Opt. Lett. **25,** 111 (1999).
8. Z. Chen, T. E. Milner, S. Srinivas, X. Wang, A. Malakzali, M. J. C. van Gemert, and J. S. Nelson, Opt. Lett. **22,** 1119 (1997).
9. W. Drexler, U. Morgner, F. X. Kartner, C. Pitris, S. A. Boppart, X. D. Li, E. P. Ippen, and J. G. Fujimoto, Opt. Lett. **24,** 1221 (1999).
10. A. F. Fercher, C. K. Hitzenberger, M. Sticker, E. Moreno-Barriuso, R. Leitgeb, W. Drexler, and H. Sattmann, Opt. Commun. **185,** 57 (2000).
11. S. Bourquin, V. Monterosso, P. Seitz, and R. P. Salathé, Opt. Lett. **25,** 102 (2000).
12. E. Beaurepaire, A. C. Boccara, M. Lebec, L. Blanchot, and H. Saint-Jalmes, Opt. Lett. **23,** 244 (1998).
13. A. Dubois, L. Vabre, A. C. Boccara, and E. Beaurepaire, Appl. Opt. **41,** 805 (2002).
14. K. K. Bizheva, A. M. Dums, and D. Boas, in *Waves and Imaging Through Complex Media*, P. Sebbah, ed. (Kluwer Academic, Dordrecht, The Netherlands, 2001), p. 277.
15. A. K. Dum, V. P. Wallace, M. Coleno, and B. J. Tromberg, Appl. Opt. **39,** 1194 (2000).